

Article

Analysis of the Seismic Properties for Engineering Purposes of the Shallow Subsurface: Two Case Studies from Italy and Croatia

Federico Da Col , Flavio Accaino , Gualtiero Böhm  and Fabio Meneghini Istituto Nazionale di Oceanografia e di Geofisica Sperimentale-OGS, 34010 Sgonico, Italy;
faccaino@ogs.it (F.A.); gbohm@ogs.it (G.B.); fmeneghini@ogs.it (F.M.)

* Correspondence: fdacol@ogs.it

Featured Application: Civil Engineering, Seismic Characterization.

Abstract: We present two case studies of the application of seismic surveys to estimate the elastic properties of soil and rock in the shallow subsurface. The two sites present very different geological characteristics. The first test site is a town on the Croatian coast, not far from the city of Split, built on hard rock, where we acquired three seismic lines. The second site is located in the outskirts of the city of Ferrara, in Italy, in an alluvial plain, where two lines were acquired. In both sites, for detailed characterization, we acquired surface-, compressional- and shear-waves, further distinguishing the latter between horizontally (SH) and vertically (SV) polarized wavefields. We processed the data by performing a Multichannel Analysis of Surface Waves to compute a preliminary one-dimensional shear wave velocity profile. Then, we performed first-break tomography to compute P-, SH- and SV-velocity profiles. Such unusual acquisition allowed us to compute not only basic engineering parameters such as the equivalent shear-wave velocity of the first 30 m of subsurface (V_{S30}) from the SH profiles but also other useful parameters such as the V_P/V_S and estimate the anisotropy of the medium thanks to the V_{SV}/V_{SH} . Given the level of detail of the results and their engineering value, we conclude that the method of investigation we applied in the two test sites is a valuable tool for characterizing the shallow subsurface.

Keywords: geophysical surveying; seismic tomography; geotechnical characterization

Citation: Da Col, F.; Accaino, F.; Böhm, G.; Meneghini, F. Analysis of the Seismic Properties for Engineering Purposes of the Shallow Subsurface: Two Case Studies from Italy and Croatia. *Appl. Sci.* **2022**, *12*, 4535. <https://doi.org/10.3390/app12094535>

Academic Editors: Andrea Chiozzi,
Elena Benvenuti and Željana Nikolić

Received: 30 March 2022

Accepted: 21 April 2022

Published: 29 April 2022

Publisher's Note: MDPI stays neutral with regard to jurisdictional claims in published maps and institutional affiliations.



Copyright: © 2022 by the authors. Licensee MDPI, Basel, Switzerland. This article is an open access article distributed under the terms and conditions of the Creative Commons Attribution (CC BY) license (<https://creativecommons.org/licenses/by/4.0/>).

1. Introduction

Geotechnical characterization of the shallow geological structures of a site is an essential tool to evaluate the response of the terrain to a macroseismic event. Typically, the geotechnical properties can be estimated by analyzing samples in a laboratory [1] or with in situ measurements such as the core penetration test and the load-bearing test.

However, these have the main disadvantage that they only provide a punctual estimation of the parameters. For this reason, geophysical surveys are becoming increasingly popular in seismic engineering thanks to their ability to accurately compute the main geotechnical parameters of the terrain and therefore its ability to amplify the seismic waves over a relatively wide area [2]. Specifically, the seismic method is able to evaluate the seismic velocities of the medium, which are a proxy for its elastic moduli [3]. More precisely, the seismic velocities are related to the bulk and shear moduli of the terrain, which describe the stiffness of the medium and therefore its ability to amplify seismic waves [4]. Based on this, in the past several decades, seismologists have established the vital importance of near-surface shear-wave velocity characterization both from a theoretical [5] and observational point of view [6]. Legislation followed these studies, and currently, the most commonly used geotechnical parameter is the equivalent shear-wave velocity of the first 30 m of subsoil (V_{S30}) [7–9]. The most widely used geophysical method to compute V_{S30} is

the Multichannel Analysis of Surface Waves (MASW) [10]. Technically, MASW relies on the dispersive behavior of the surface waves and consists in extracting a dispersion curve from a recorded seismogram and inverting it, obtaining a 1D shear-wave velocity profile. Yust et al. (2018) [11] show that the method is able to estimate accurately V_s profiles and therefore compute the V_{S30} with a relatively small error. Another method that relies on the surface waves is the Horizontal to Vertical Spectral Ratio (HVSr, [12]). The method consists in processing the data from 3C single-station data by computing the ratio between the horizontal and vertical spectra and thereby extracting a 1D shear-wave velocity profile together with the resonant frequency of the terrain.

A method that is gaining popularity is the travel-time tomography of first breaks on an SH active seismic survey [13,14]. The main advantage of this method is that it provides a 2D (potentially even 3D) S-wave velocity profile and therefore a computation of the V_{S30} along the entire seismic line.

A more accurate characterization of the shallow subsurface, beyond the computation of the V_{S30} , can be of high interest for engineers. For instance, from the computation of Poisson's ratio or V_P/V_S , information regarding the fracturing of the rocks [1] and its fluid saturation [15] can be inferred.

In this work, we present the application of an innovative survey technique in two case studies from two very different sites. The first was recorded along the roads of a small town lying on hard rock in the area of Split in Croatia. The second case study consists of a dataset recorded in an alluvial plain in an intensively cultivated countryside close to the city of Ferrara. The novelty of the method proposed lies in the fact that we recorded separately compressional- and shear-wavefields, distinguishing in the latter between the components orthogonal (SH) and parallel (SV) to the seismic line. In fact, while integrating P- and SH-waves is increasingly popular in the near-surface geophysics community [16,17], the distinction between SH- and SV-wavefields is much rarer. Seismologists performed several numerical simulations [18] and analyzed field data [19] aiming at the study of shear-wave splitting and anisotropy, but hardly any field example using controlled sources can be found in the literature.

In the same surveys, data specifically for surface-wave analysis was also recorded. The final aim of our analyses is to provide detailed engineering information of the shallow subsurface without invasive tests at a relatively large scale. Successful testing of the method in two such different locations should allow us to confirm whether the method is replicable in most situations.

2. Geological Context

The Croatian site lies in the village of Kaštela Kambelovac, which is a town lying on the shores of the homonymous bay, just northwest of the city of Split. Geologically, the Bay lies in a compressional environment [20], where the rocks are subject to strong thrusting and folding. This caused the thrusting of the Senonian limestone on top of the Eocene flysch [21,22]. The town therefore is built on top of such flysch, the thickness of which has been estimated to be several hundreds of meters and the composition of which is known to be mainly of alternating layers of marls and calcarenites/calcirudites [23]. Previous geological and geotechnical investigations in the area showed that the bedding of the flysch is subvertical because of the tectonic compressional context. More detailed geological information about the Croatian site can be found in [24].

As for the Italian site, the acquisition took place in the southeastern suburbs of the city of Ferrara, in the central Po Valley, an alluvial, subsiding plain. Specifically, the area where the studies were carried out lies at the heart of such a plain, filled with olocenic sediments of marine, lagunal and riverine origin [25]. These are horizontally layered and composed of sand mixed with clay and silt, the proportion of which is variable both depending on the location and on the depth. These sediments are often not consolidated, giving place to phenomena of liquefaction during macroseismic events [26]. At the base of the olocenic sediments, located at approximately 1000 m depth, lie the so-called "Ferrara folds", pre-

pleistocene rocks folded by the Appennine orogeny (“Buried Appennine” [27]). In fact, tectonically, the area lies at the margin of the compressional environment that created the Appennine mountain range.

3. Data Acquisition

In both sites, we acquired three wavefields separately (P, SH and SV). To do this, we used as source a wheelbarrow-mounted vibrator, which is capable of generating both P- and S-waves, reorienting it orthogonal and parallel to the line to generate SH- and SV-waves, respectively. As for the receivers, we used 10 Hz vertical geophones to record the P-waves and 14 Hz horizontal geophones to record the S-waves. The latter were re-oriented to record SH and SV, respectively, orthogonal and parallel to the survey line. We vibrated twice at each shot point, to perform stacking of the seismograms and therefore increase the signal–noise ratio.

3.1. Ferrara Site

We acquired two high-resolution seismic lines, the location of which can be seen in Figure 1a, while the UTM coordinates of the two lines are reported in Table 1. For both lines, we deployed 150 active channels, spaced every 2 m, and we shot every 4 m. The length of both lines is therefore approximately 300 m.

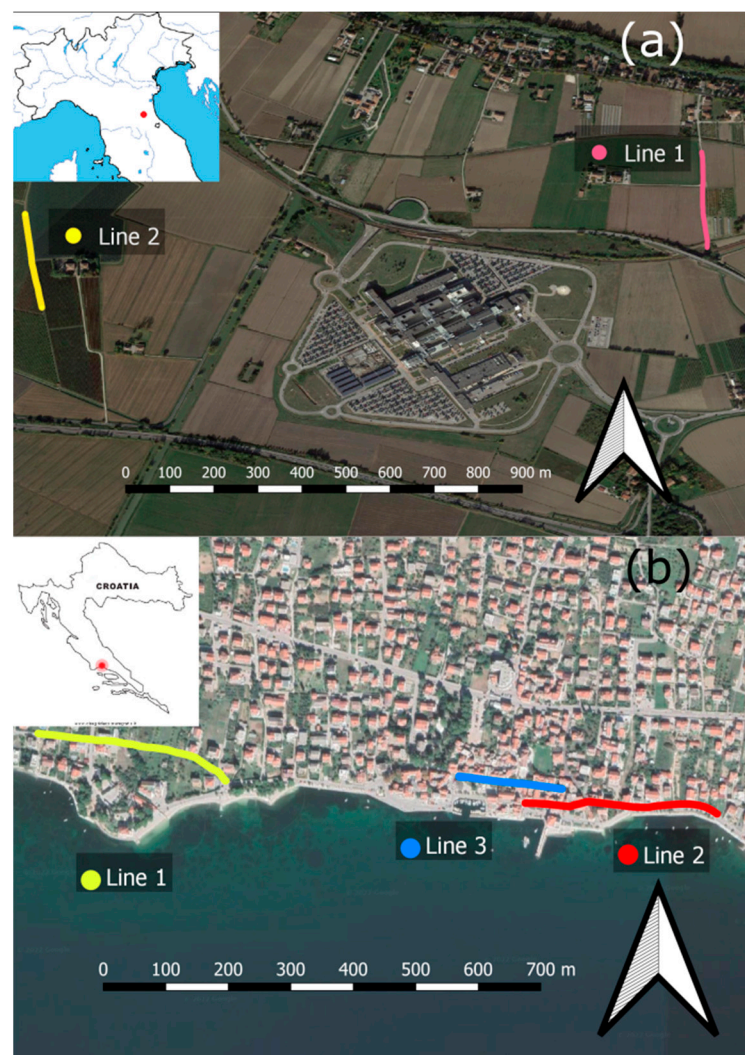


Figure 1. (a) Location of the lines acquired in the area of Ferrara, Italy. (b) Location of the lines acquired in Kaštela, Croatia. Images created on Google Earth Pro on 30 March 2022.

Table 1. UTM coordinates of the first and last receiver of each acquired seismic line.

Line Name	First Rec. N	First Rec. E	Last Rec. N	Last Rec. E	UTM Zone
Ferrara Line 1	4964800	713828	4964503	713850	32
Ferrara Line 2	4964552	712300	4964258	712347	32
Kastela Line 1	4822696	611466	4822770	611167	33
Kastela Line 2	4822643	612232	4822660	611943	33
Kastela Line 3	4822683	611984	4822703	611821	33

Along Line 1 (highlighted in red in Figure 1a), we acquired surface-wave data by deploying 48 4.5 Hz receivers, which were spaced every 4 m. As a source, we used a 100 kg weight-drop. We shot four times: twice at the beginning and twice at the end of the line.

The data of Line 1 were acquired along a gravel road. The main sources of noise were the agricultural activities ongoing in the nearby fruit farms (tractors, walking, irrigation pumps) and the car traffic.

The data of Line 2 were acquired in a fruit farm along a line of pear trees. Therefore, the geophones were planted in the soft soil. The main sources of noise are, similarly to Line 1, the activities going on in the fruit farm, including tractors and irrigation pumps.

3.2. Kaštela Site

We acquired three seismic lines along the roads of the village, planting the sensors in holes drilled in the tarmac. The details of the survey are outlined in [14], and the location of the lines can be seen in Figure 1b, while the UTM coordinates are reported in Table 1. Line 1 and 2 are 300 m long, while Line 3 is 150 m long. The receiver spacing in all lines is 2 m, and the shot spacing is 4 m. It is to be noted that during the acquisition of Line 1 and Line 2, traffic was quite intense in the village, and the weather was windy and even rainy at times. On the other hand, Line 3 was less affected by traffic noise, and the weather was fine.

4. Processing Methods

Multichannel Analysis of Surface Waves [10] provided information only on the Ferrara site, as no dispersive event could be identified in the Kaštela dataset, which was probably due the presence of tubes or other voids just below the road.

In Figure 2a, we show the frequency-wavenumber (f - k) spectrum of the Ferrara dataset, from which we picked the most energetic linear (i.e., dispersive) event to compute the dispersion curve shown in Figure 2b. The frequency range is from 3.5 to 15 Hz, giving a maximum wavelength of 58 m, i.e., a penetration depth of 29 m ($\lambda/2$, where λ is the wavelength). Finally, we inverted such a dispersion curve using the neighborhood algorithm in the GeoPsy software [27]. The initial model consists of three layers + Halfspace, the properties of which are described in Table 2. One million profiles were computed; in Figure 2c, we show the 500 best—that is, those generating a synthetic dispersion curve having the lowest misfit with respect to the picked one.

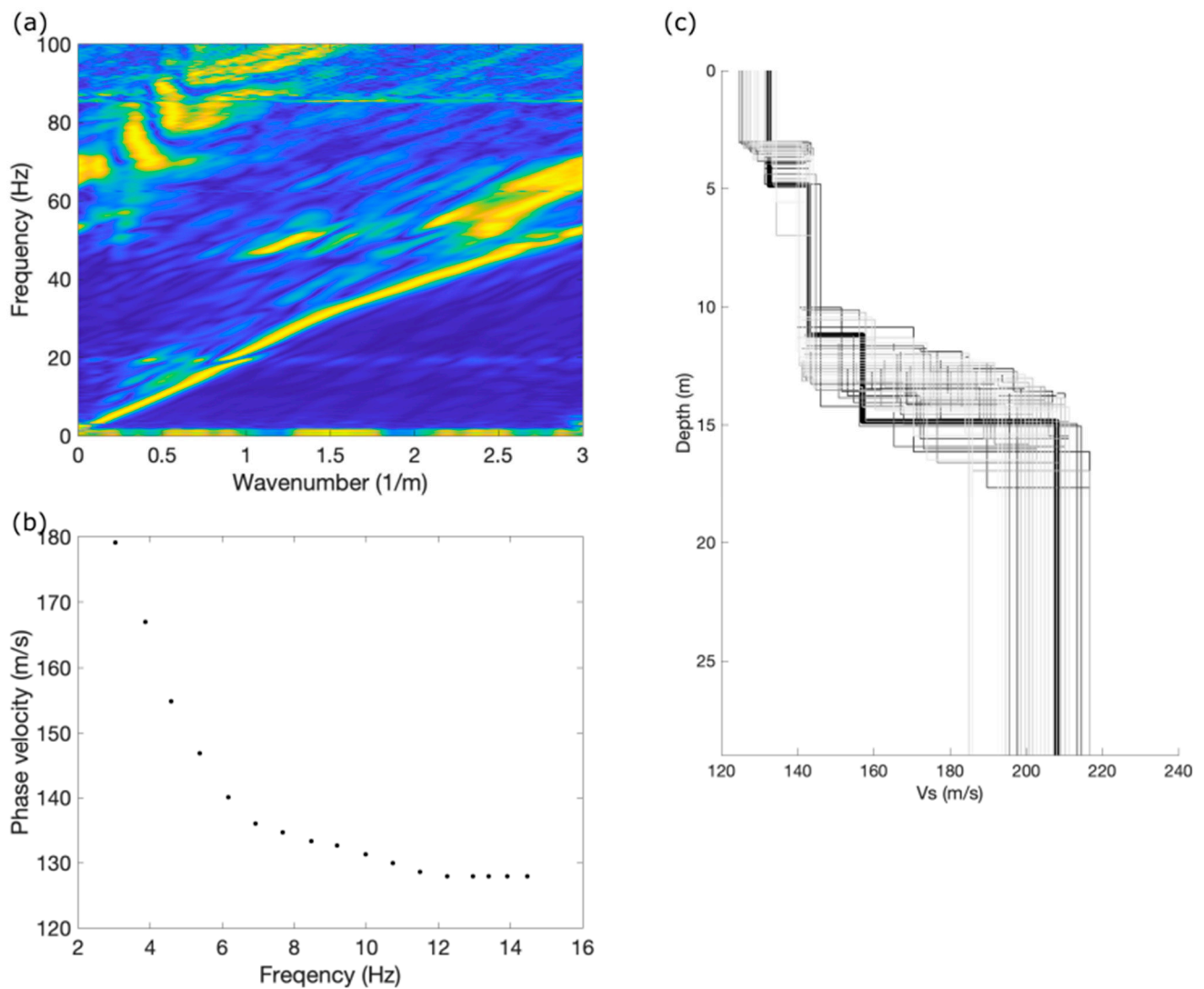


Figure 2. (a) f-k spectrum. (b) Dispersion curve. (c) The 1000 best fitting S-wave velocity profiles. The color of the lines represents the misfit, as indicated in the color bar.

Table 2. Properties of the initial model used for the inversion of the surface waves.

Layer Number	Thickness	Vs	Density
1	3–15 m	100–200 m/s	2000 kg/m ³
2	3–15 m	120–220 m/s	
3	3–15 m	140–240 m/s	
Halfspace		150–250 m/s	

We performed first break tomography on all the lines for all of the wavefields. Before this, some pre-processing was performed. Specifically, to increase the signal-to-noise ratio, for each shot, we applied a predictive deconvolution to the uncorrelated signals as in [28]. Furthermore, to remove random noise, we stacked in the time domain the seismograms relative to the same shot point.

The first breaks were manually picked on the seismograms. Examples of first-break picking can be seen in Figure 3.

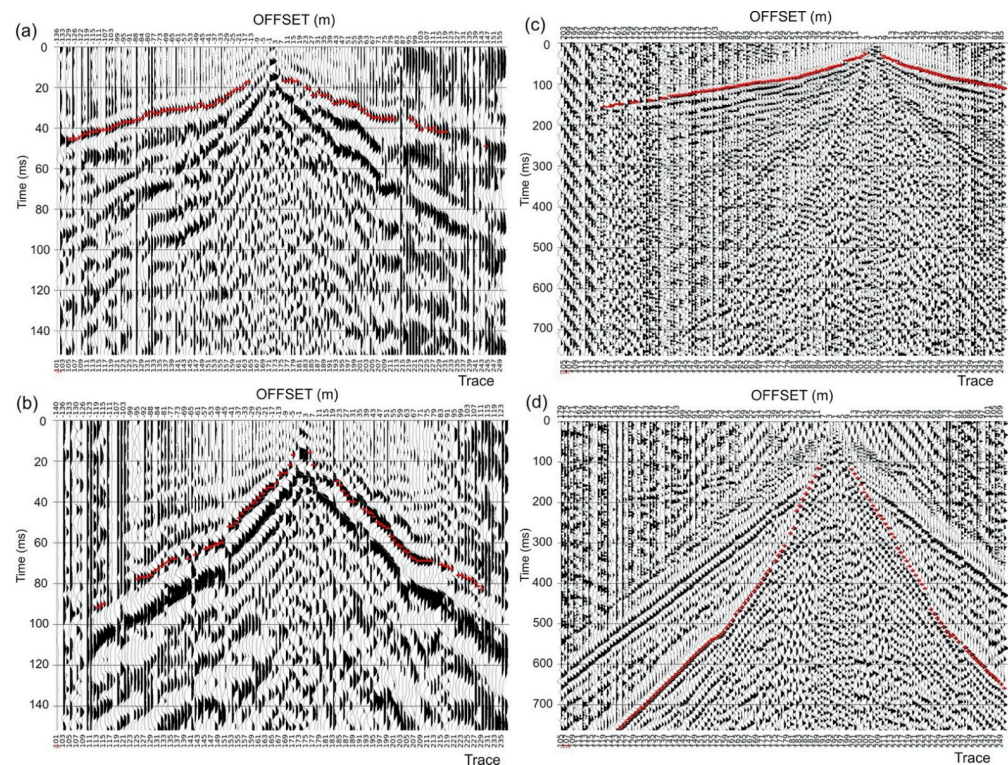


Figure 3. Examples of first-break picking on common shot gathers. Highlighted in red are the picked travel times. (a) P-waves from the Croatian site. (b) SH-waves from the Croatian site. (c) P-waves from the Italian site. (d) SH-waves from the Italian site.

Then, the travel times were inverted with Cat3D software [29], which is a tomographic package developed at the National Institute of Oceanography and Applied Geophysics-OGS that uses a ray-tracing algorithm based on a minimum time principle and SIRT (Simultaneous Iterative Reconstruction Technique) as an inversion method [30].

5. Results and Discussion

In Figure 4, we show the velocity profiles from the tomographic inversion of all wavefields relative to the three lines acquired in Kaštela, while in Figure 5, we show those relative to the two lines acquired in Ferrara. The two velocity profiles show very different features. In Kaštela, below a slower weathered layer, the velocity rapidly increases to 4.5 km/s and 3.0 km/s for P- and S-waves, respectively. Furthermore, we observe an overall increase in the velocities in the eastern lines (Lines 2 and 3) compared to the western line 1. In Figure 4d–f, we show the SH-velocity profiles and the corresponding V_{S30} . Since the velocity is >800 m/s along all three profiles, we conclude that the soil can be classified as A-class following the Eurocode-8 provisions [9]. In the bottom-right corner of each velocity profile, the mean RMS error is reported. All profiles present a mean RMS lower than 5%, except for the P-wave profile of line 2. This is probably due to the low signal-to-noise ratio of the data caused by the rainfall during the acquisition. Having said this, all other profiles show low mean RMS and can therefore be considered reliable.

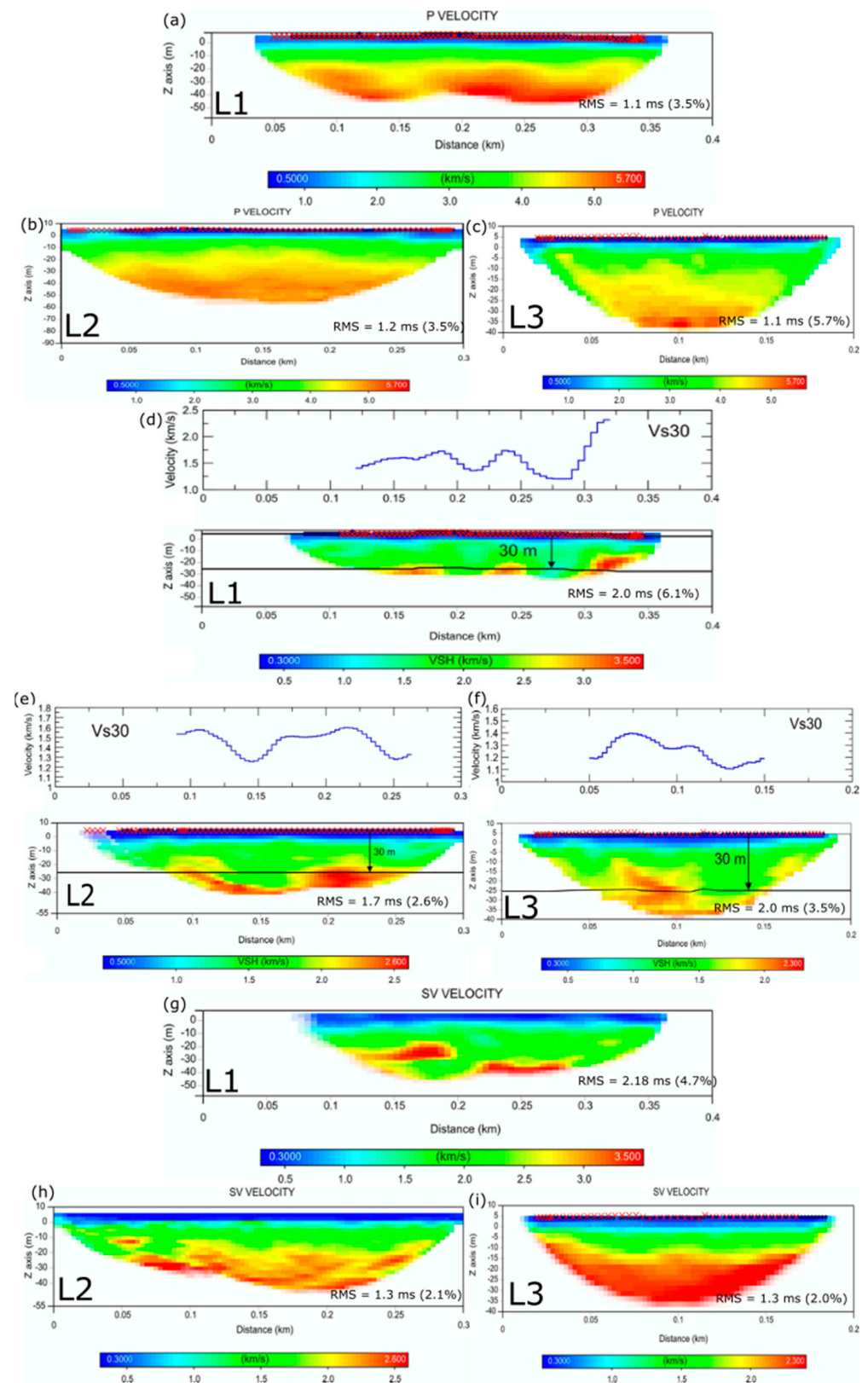


Figure 4. Results of the tomographies in Croatia; in the bottom-right corner, the value of the mean RMS error is shown. (a) Line 1, P-waves, (b) Line 2, P-waves, (c) Line 3, P-waves, (d) Line 1, SH-waves and V_{S30} , (e) Line 2 SH-waves and V_{S30} , (f) Line 3 SH-waves and V_{S30} , (g) Line 1 SV-waves, (h) Line 2 SV-waves, (i) Line 3 SV-waves.

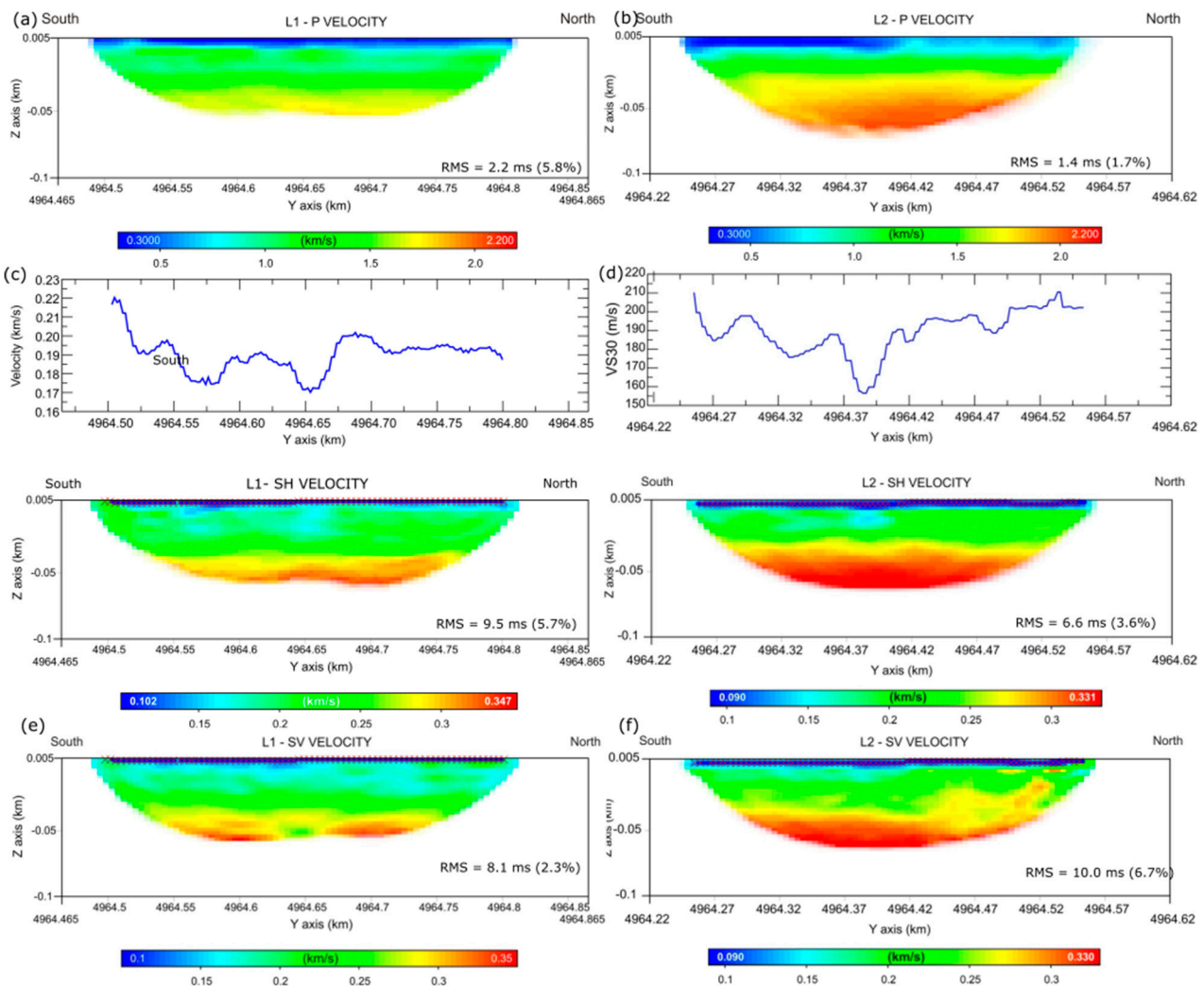


Figure 5. Velocity profiles from the Italian site; in the bottom-right corner, the value of the mean RMS error is shown. (a) Line 1 P-waves, (b) Line 2 P-waves, (c) Line 1 SH-waves with V_{S30} , (d) Line 2 SH-waves with V_{S30} , (e) Line 1 SV-waves, (f) Line 2 SV-waves.

In Figure 4, we show the velocity profiles relative to all wavefields for the two lines acquired in Ferrara. We observe a horizontal layering of the sediments, which is typical of alluvial plains. The highest velocities are reached in Line 2, where they exceed 2 km/s and 0.3 km/s for P- and S-waves, respectively. The V_{S30} is shown in Figure 4c,d, and it shows values for which the soil can be identified as C-class ($V_{S30} > 180$ m/s) following the Eurocode-8 provisions [9], matching the estimates performed in the area by previous large-scale studies [31]. This value and the velocity profile at the center of the line (where the 1D S-wave velocity profile from the MASW is ideally located) is compatible with the results of the inversion of the surface waves, confirming the reliability of our results. The sharp transition at approximately 3 m depth from blue to green in both P-wave velocity profiles most likely indicates the water table. This is consistent with previous geotechnical investigations in the area [32]. Similarly to Figure 4, the mean RMS error is shown in the bottom-right corner of each velocity profile. The values are quite variable, depending on the signal-to-noise ratio of the datasets, which depended on the amount of activities ongoing in the fields. Having said this, they usually show quite a low value, in the range of 5%, and therefore, the velocity profiles can be considered reliable.

Further information about the sites can be obtained by computing the V_P/V_S ratio (proxy for Poisson's ratio). In Figure 6a–c, we show the V_P/V_S profiles relative to the three lines acquired in Croatia, while in Figure 6d,e, we show those relative to the lines acquired

in Italy. The profiles acquired in Croatia show an overall increase in the V_P/V_S ratio in the eastern lines (especially Line 3) compared to the western line. This indicates a more fractured medium that is possibly saturated with water. As for the Italian site, the V_P/V_S ratio is very high in both profiles, reaching a maximum in Line 2. The sharp increase in both lines at a depth of approximately 3 m confirms the position of the water table. Furthermore, such high V_P/V_S probably indicate the presence of water-saturated unconsolidated clay sediments.

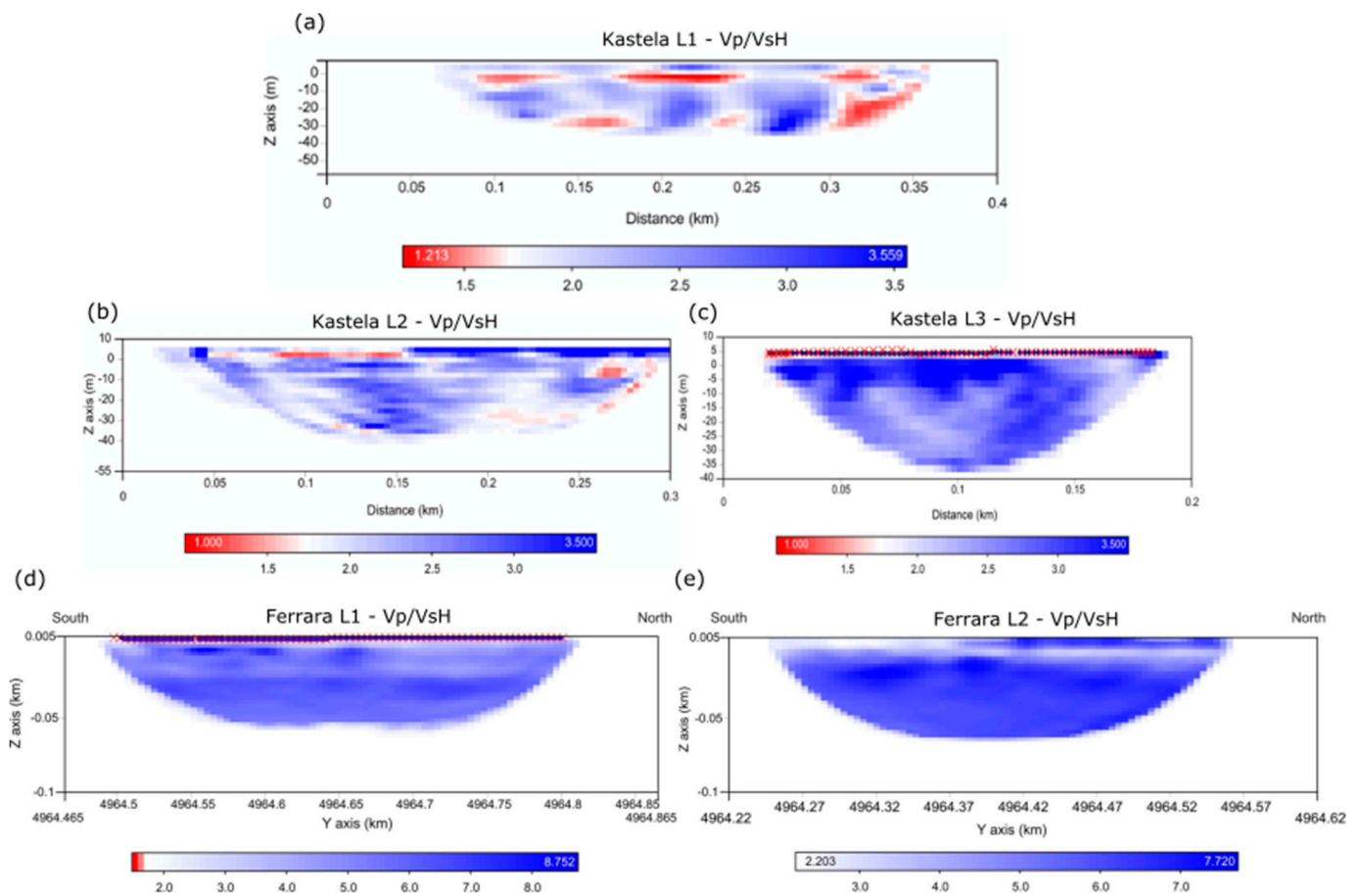


Figure 6. V_P/V_{SH} (a) Kaštela Line 1. (b) Kaštela Line 2. (c) Kaštela Line 3. (d) Ferrara Line 1. (e) Ferrara Line 2.

In Figure 7, we show profiles of the V_{SV}/V_{SH} . In the Croatian site, shown in Figure 7a–c, the presence of anisotropy is due to the layering of the Eocene flysch [14]. From the geometrical considerations applied to the raypaths, it is possible to estimate the bedding angles (dip and strike), as shown in [14]. As for the Italian site, shown in Figure 7d,e the presence of anisotropy confirms that the sediments are composed of horizontal layers of clay and silt, which are known for producing anisotropy [33,34]

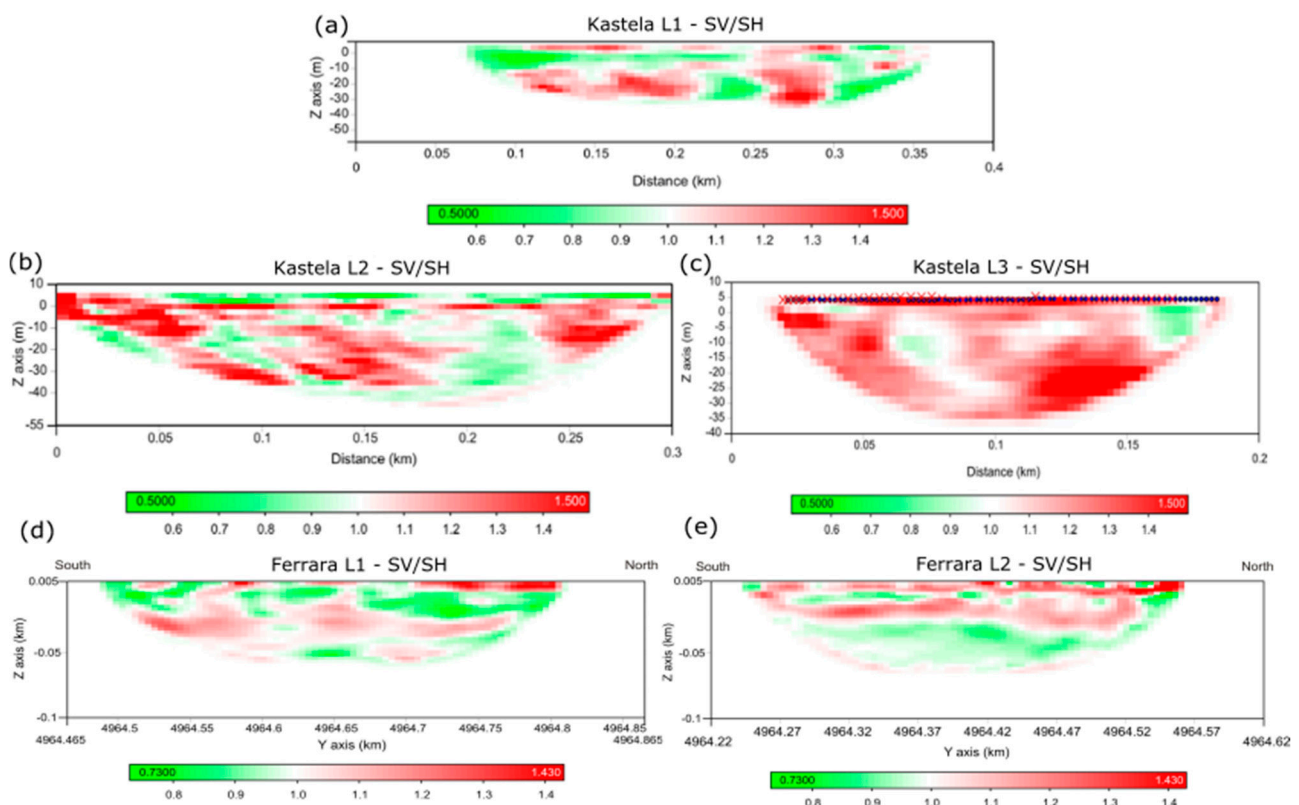


Figure 7. V_{SV}/V_{SH} (a) Kaštela Line 1. (b) Kaštela Line 2. (c) Kaštela Line 3. (d) Ferrara Line 1. (e) Ferrara Line 2.

6. Conclusions

We presented two case studies from two very different sites in order to validate the method in such different circumstances. The first consisted of three high-resolution seismic lines acquired along the roads of a village built on hard rock in Croatia. The second consisted of two high-resolution seismic lines acquired in a cultivated area in northern Italy. In both cases, we acquired P-waves as well as S-waves, the latter in two different polarizations: parallel (SV) and orthogonal (SH) to the seismic line. Furthermore, surface-waves were acquired in the two sites. However, in Croatia, no dispersive event could be identified and therefore no results could be obtained. This highlights the importance of acquiring SH-waves. We then performed first break tomography on all lines, for all wavefields.

The results output by the presented survey method are of high value for engineering purposes, as well as for the overall geological and geotechnical characterization of the investigated areas. Specifically, from an engineering point of view, the sites were classified based on their V_{S30} as required by the current legislation. The method allows to investigate also other important properties of the subsurface, such as the V_P/V_S and the anisotropy of the medium. From the former, it is possible to infer the fracturing of the medium and its water saturation (i.e., the position of the water table). From the latter in the Croatian site, it was possible to compute the dip and strike angles of the bedding of the flysch, providing therefore a geologically valuable information, while in the Italian site, it confirmed the silty/clay composition of the sediments and their horizontal layering.

The method proposed is non-invasive, replicable and relatively cheap, as the acquisition required only 2–3 days for each seismic line. Furthermore, it provides an in-depth characterization of the composition of the subsurface up to a depth of several tens of meters without the need for expensive procedures such as drilling and coring. Finally, these parameters are given along entire profiles, a few hundred meters long, making it attractive for the extensive characterization of geologically heterogeneous areas.

Given the value of the results and all the above considerations, we conclude that the method proposed is an optimal tool to perform an in-depth characterization of the shallow layers of the subsurface.

Author Contributions: Conceptualization, F.A., F.D.C. and G.B.; methodology, F.A. and G.B.; software, F.D.C. and G.B.; validation, F.D.C., G.B. and F.A.; formal analysis, G.B. and F.D.C.; investigation, F.A., F.D.C. and G.B.; resources, F.A. and F.M.; data curation, F.M.; writing—original draft preparation, F.D.C.; writing—review and editing, F.D.C.; visualization, F.D.C., G.B. and F.M.; supervision, F.A.; project administration, F.A.; funding acquisition, F.A. All authors have read and agreed to the published version of the manuscript.

Funding: The research presented in this paper has been carried out within the PMO-GATE (Preventing, Managing and Overcoming Natural-Hazards Risks to mitiGATE economic and social impact) project. Such project falls in the Interreg Italy-Croatia programme of the European Commission under project id 10046122.

Institutional Review Board Statement: Not applicable.

Informed Consent Statement: Not applicable.

Data Availability Statement: The data presented in this study are available on request from the corresponding author.

Acknowledgments: We thank the crew involved in the two data acquisitions, in the names of Stefano Maffione, Gino Cristofano, Massimo Lovo and Andrea Schleifer. Special thanks also to Zeljana Nikolic of the University of Split, who gave us important feedback on the results we obtained. A final thank to the Municipalities both of Ferrara and Kaštela, who gave important help with the logistics.

Conflicts of Interest: The authors declare no conflict of interest.

References

1. Lancellotta, R. *Geotechnical Engineering*; CRC Press: London, UK, 2008.
2. Cardarelli, E.; Cercato, M.; De Donno, G. Characterization of an earth-filled dam through the combined use of electrical resistivity tomography, P-and SH-wave seismic tomography and surface wave data. *J. Appl. Geophys.* **2014**, *106*, 87–95. [[CrossRef](#)]
3. Ansal, A.; Kurtulus, A.; Tönük, G. Seismic microzonation and earthquake damage scenarios for urban areas. *Soil Dyn. Earthq. Eng.* **2010**, *30*, 1319–1328. [[CrossRef](#)]
4. Aki, K.; Richards, P.G. *Quantitative Seismology*; W.H. Freeman: San Francisco, CA, USA, 1980; Volume 1.
5. Stein, S.; Wysession, M. *An Introduction to Seismology, Earthquakes and Earth Structure*; Blackwell Publishing Ltd.: Malden, MA, USA, 2009.
6. Borcherdt, R.D. Estimates of site-dependent response spectra for design (methodology and justification). *Earth Spectra* **1994**, *10*, 617–654. [[CrossRef](#)]
7. Borcherdt, R.D. Simplified site classes and empirical amplification factors for site-dependent code provisions: NCEER, SEADC, BSSC. In Proceedings of the Workshop on Site Response during Earthquakes and Seismic Code Provisions, Los Angeles, CA, USA, 18–20 November 1992.
8. Dobry, R.; Borcherdt, R.D.; Crouse, C.B.; Idriss, I.M.; Joyner, W.B.; Martin, G.R.; Seed, R.B. New site coefficients and site classification system used in recent building seismic code provisions. *Earthquake Spectra* **2000**, *16*, 41–67. [[CrossRef](#)]
9. Sabetta, F.; Bommer, J. Modification of the spectral shapes and subsoil conditions in Eurocode 8. In Proceedings of the 12th European Conference on Earthquake Engineering, London, UK, 9–13 September 2002.
10. Park, C.B.; Miller, R.D.; Xia, J. Multichannel analysis of surface waves. *Geophysics* **1999**, *64*, 800–808. [[CrossRef](#)]
11. Yust, M.B.S.; Cox, R.B.; Cheng, T. Epistemic Uncertainty in Vs Profiles and Vs30 Values Derived from Joint Consideration of Surface Wave and H/V Data at the FW07 TexNet Station. In *Geotechnical Earthquake Engineering and Soil Dynamics V: Seismic Hazard Analysis, Earthquake Ground Motions, and Regional-Scale Assessment*; American Society of Civil Engineers: Reston, VA, USA, 2018; pp. 387–399.
12. Nakamura, Y. A method for dynamic characteristics estimation of subsurface using microtremor on the ground surface. *Railway Tech. Res. Inst. (Q. Rep.)* **1989**, *30*.
13. Chan, J.H.; Catchings, R.D.; Goldman, M.R.; Criley, C.J. *VS30 at Three Strong-motion Recording Stations in Napa and Napa County, California—Main Street in Downtown Napa, Napa Fire Station Number 3, and Kreuzer Lane—Calculations Determined From s-Wave Refraction Tomography and Multichannel Analysis of Surface Waves (Rayleigh and Love)*; US Geological Survey: Reston, VA, USA, 2018.
14. Da Col, F.; Accaino, F.; Böhm, G.; Meneghini, F. Characterisation of shallow sediments by processing of P, SH and SV wavefields in Kaštela (HR). *Eng. Geol.* **2021**, *293*, 106336. [[CrossRef](#)]

15. Uhlemann, S.; Hagedorn, S.; Dashwood, B.; Maurer, H.; Gunn, D.; Dijkstra, T.; Chambers, J. Landslide characterization using P- and S-wave seismic refraction tomography—The importance of elastic moduli. *J. Appl. Geophys.* **2016**, *134*, 64–76. [[CrossRef](#)]
16. Chen, J.; Zelt, C.A.; Jaiswal, P. Detecting a known near-surface target through application of frequency-dependent traveltimes tomography and full-waveform inversion to P- and SH-wave seismic refraction data. *Geophysics* **2017**, *82*, R1–R17. [[CrossRef](#)]
17. Wang, C.; Shi, Z.; Yang, W.; Wei, Y.; Huang, M. High-resolution shallow anomaly characterization using cross-hole P- and S-wave tomography. *J. Appl. Geophys.* **2022**, *201*, 104649. [[CrossRef](#)]
18. Fishman, K.L.; Ahmad, S. Seismic response for alluvial valleys subjected to SH, P and Sv waves. *Soil Dyn. Earthq. Eng.* **1995**, *14*, 249–258. [[CrossRef](#)]
19. Yong-Gang, L. Seismic wave propagation in anisotropic rocks with applications to defining fractures in earth crust. In *Rock Anisotropy, Fracture and Earthquake Assessment*; Walter de Gruyter: Berlin, Germany, 2016.
20. Herak, M. *A New Concept of Geotectonics of the Dinarides*; Jugoslavenska Akademija Znanosti i Umjetnosti: Zagreb, Croatia, 1986.
21. Marincic, S.; Magas, N.; Borovic, I. *Osnovna Geoloska Karta SFRJ 1: 100.000, List Split i Pripadaju i Tumac Karte, K33-21*; Institute of Geology: Zagreb, Croatia, 1973.
22. Buljan, R.; Pollack, D.; Pest, D. Engineering geological properties of the rock mass along the Kastela Bay sewage system. *Geol. Soc. Lond.* **2006**, *740*, 467–477.
23. Babic, L.; Zupancic, J. Evolution of a river-fed foreland basin fill: The north Dalmatia flysch revisited (Eocene, outer dinarides). *Nat. Croat.* **2008**, *17*, 357–374.
24. Gargini, A.; Bondesan, M.; Pasini, M.; Messina, A.; Piccinini, L.; Zanella, A.; Oddone, E. *Supporto Tecnico Geologico-Idrologico Alla Procedura di Valutazione e Sostenibilità Ambientale per Il Nuovo Piano Regolatore del Comune di Ferrara—Zona via Bologna—Direttrice per Cona. Relazione n. 1/03.01*; Comune di Ferrara: Ferrara, Italy, 2003.
25. Fontana, D.; Lugli, S.; Marchetti Dori, S.; Caputo, R.; Stefani, M. Sedimentology and composition of sands injected during the seismic crisis of May 2012 (Emilia, Italy): Clues for source layer identification and liquefaction regime. *Sediment. Geol.* **2015**, *325*, 158–167. [[CrossRef](#)]
26. Pieri, M.; Groppi, G. *Subsurface Geological Structure of the Po Plain, Italy. Pubbl.414. P.F. Geodinamica*; C.N.R.: Milano, Italy, 1981; pp. 1–23.
27. Wathelet, M. An improved neighborhood algorithm: Parameter conditions and dynamic scaling. *Geophys. Res. Lett.* **2008**, *35*, L09301. [[CrossRef](#)]
28. Baradello, L.; Accaino, F. Vibroseis deconvolution: A comparison of pre and post correlation vibroseis deconvolution data in real noisy data. *J. Appl. Geophys.* **2013**, *92*, 50–56. [[CrossRef](#)]
29. Böhm, G.; OGS Research Group. *Cat3D. Computer Aided Tomography for 3-D Models. User Manual*; OGS: Trieste, Italy, 2014.
30. Stewart, R. Exploration Seismic Tomography: Fundamentals. In *Course Note Series*; Domenico, S.N., Ed.; SEG—Society of Exploration Geophysicists: Tulsa, OK, USA, 1993; Volume 3.
31. Condotta, M. *Progetto di Adeguamento Funzionale del Sistema Irriguo Della Valli Giralda, Gaffaro e Falce in Comune di Codigoro (FE). Relazione Geologica e Geotecnica. Elaborato 1.2*; Consorzio di Bonifica Pianura di Ferrara: Ferrara, Italy, 2011.
32. Rossi, F.; Tumiati, D.; Bassi, A.; Perelli, P. *Piano Particolareggiato di Iniziativa Pubblica—Sottozona F2—Polo Ospedaliero di Cona. Rapporto di Valutazione Ambientale del Piano Particolareggiato in Località Cona di Ferrara*; Comune di Ferrara: Ferrara, Italy, 2011.
33. Wang, Z. Seismic anisotropy in sedimentary rocks. Part 2, Laboratory tests. *Geophysics* **2002**, *67*, 1348–1672. [[CrossRef](#)]
34. Sayers, C.M.; Den Boer, L.D. The elastic anisotropy of clay minerals. *Geophysics* **2016**, *81*, C193–C203. [[CrossRef](#)]